www.czasopisma.pan.pl PAN www.journals.pan.pl
Opto-Electronics Review 25 (2017) 311–317

Contents lists available at ScienceDirect

Opto-Electronics Review

journal homepage: http://www.journals.elsevier.com/opto-electronics review

An 80 Gbps multi-band access radio over fiber link with single side band optical millimeter-wave dispersion-tolerant transmission without FBG and optical filter

R.S. Asha [a,*], V.K. Jayasree [b], S. Mhatli [c]

[a] Department of Electronics, Model Engineering College, Thrikkakara, Ernakulam, Kerala, 682021, India
[b] Department of Electronics and Communication Engineering, College of Engineering, Adoor, Kerala, India
[c] SERCOM-Labs, EPT Université de Carthage, 2078, La Marsa, Tunis, Tunisia

ARTICLE INFO

Article history:
Received 25 January 2017
Received in revised form 12 June 2017
Accepted 6 July 2017
Available online 29 September 2017

Keywords:
Millimeter wave
Optical Carrier Suppression
MZM
OSNR

ABSTRACT

We are presenting a new low-cost Single Sideband (SSB) modulated Radio-over Fiber (RoF) communication system for millimeter (mm)-wave multiband wireless communication at the frequencies of 40 GHz, 80 GHz and 120 GHz. Its principle lies in the Carrier Suppressed modulation through a nested dual electrode Mach–Zehnder Modulator (MZM) and product modulator based baseband signal decomposition. In this novel method, the optical signal is decomposed into different SSB signals using a power splitter and product modulators at the base station. This proposed method uses a different technique for a baseband signal decomposition from the existing method. The proposed signal decomposition technique has reduced the nonlinearities due to the FBGs. The proposed method is compared with the existing method in terms of BER, data rate and OSNR. The simulation results disclose that our proposed scheme outperforms the existing methods at a higher data rate of 80 Gbps with a minimum BER and privileged Q factor.

1. Introduction

Current high-definition video services need higher bandwidth for wired and wireless data transmission. The millimeter (MM) wave band is a significant research topic for high-speed wireless data transfer [1]. The RoF technologies can be used to fixed and mobile end users with huge capacity, coverage, and mobility [2,3]. To get full advantages of integrated optical fiber and wireless system, the RoF technology is selected as a smart solution for the wireless network. It can improve the service area of the mm-wave band wireless signals [4,5]. The multiband modulation and transmission have been demonstrated [6,7]. The Electro-Absorption Modulator (EAM) nonlinearity, chirp and the crosstalk among three signals reduce the performance in Ref. [4]. The scheme proposed in Ref. [7] is very expensive and complicated.

Reference [8] is an emerging technology with huge communication capacity and low cost. The multiband signal's transmissions have been demonstrated in Refs. [9–19]. The multiband electrical signals are pooled and changed in to an optical signal through an Electro-absorption Modulator (EAM) [9–11]. In these methods, the optical modulator is biased at the quadrature operation point. Its performance is affected by the nonlinear behaviour of EAM. The advantage of these methods is restricted by the chirping effect, nonlinearity of the modulator and the crosstalk. A WDM optical network and a 60 GHz RoF link using single-drive Mach–Zehnder modulator (MZM) for a wavelength-division multiplexed optical network is proposed in Ref. [12].

All users can receive their data at the base stations but only two-band signals are produced. Reference [13] has proposed a method using hybrid mode-locked laser with 5 WDM channels. But it has produced the same problems as in Ref. [12]. An Arrayed Waveguide Grating (AWG) multiplexer is used to integrate the dense WDM multiband signals with a frequency spacing of 12.5 GHz [14]. But three laser sources and three modulators are used at the Central Station (CS), the system becomes expensive. Multiband signals are generated [15] by a dual-parallel MZM and a single-drive MZM based on carrier suppression and frequency shifting techniques. The method of a multiband mm-wave generation is expensive and the generated spectrum is complex. Each sideband can stimulate amplitude-fading effect.

A multiband spectrum is generated by two cascaded MZMs [16,17] with low dispersion. A DSB optical spectrum is generated from the first MZM operating in maximum transmission point. The carrier suppressed spectrum is generated from the second MZM as it is operating in minimum transmission point. Even though this method has high dispersion tolerance; an optical filter is used to convert the DSB modulated optical signal to the SSB modulated signal. A duplex RoF system is proposed with downlink frequencies at

* Corresponding author.
E-mail address: ashars@mec.ac.in (R.S. Asha).

http://dx.doi.org/10.1016/j.opelre.2017.07.001
1896-3757/

60 GHz, 20 GHz and baseband signal through a single MZM [18]. The same problems are found here as [15] with intricate spectrum. In Ref. [19], bidirectional three multi band mm-waves are generated. It consists of a cascade connection of a modulator and MZM. Several coherent waves are used to generate downlink mm-waves. Due to the chromatic dispersion, the data carrying light waves have fading effect and degrade the signal performance.

Here, we have proposed a novel RoF multiband communication with 40 GHz, 80 GHz and 120 GHz mm-wave signals. The optical signal is produced by a nested MZM and an optical source at the CS. One MZM is biased at the quadrature point and other is biased at the null point. The output spectrum consists of four frequencies with an equal frequency difference of 40 GHz. The downlink data is carried by one carrier, but the others are unmodulated frequencies. The mm-waves at 40 GHz, 80 GHz and 120 GHz are obtained via photodetector, power splitter and three product modulators at the base station (BS). The uplink optical carrier is selected from one of the three unmodulated sidebands. The simulation results assure the advantages of our proposed mm-wave multiband wireless communication.

Compared with the previous reports [9–23], our method is potentially novel with several advantages. This method has one mm-wave generator and a nested MZM at the CS and makes a cost-competent CS. The downstream data is carried by one carrier signal, so the chromatic dispersion is significantly reduced. Compared with the report [24], this method can reduce the cost of CS in the optical domain since no FBGs and optical filters are used in the circuit. This method is used a novel baseband decomposition method at the BS. This proposed method is also used at a higher data rate of 80 Gbps. It offers more signal power about 15 dB than the existing method. Q factor is in the range of 14 dB. BER is also below from 10^{-20} for two bands. Simulation results show that the proposed method can perform better in terms of BER, Q factor, OSNR, and data rate.

This paper is organized as follows. The theoretical analysis of the proposed multiband wireless access RoF transmission is explained in Section 2. Section 3 deals with the RoF link with 80 Gb/s mm-wave wireless access signals with a simulation platform. Finally, section 4 concludes the work.

2. Operation Principle

The block diagram of the proposed multiband RoF transmitter is shown in Fig. 1. The continuous wave (CW) laser, generated an optical signal is represented by $E_c(t) = E_c \exp(j\omega t)$, is spiltted into two signals by the nested MZM. After that the two signals are independently applied into two inner-MZMs of the central MZM. Figure 1 shows that the two leads of the upper inner-MZM-1 are operated by a local oscillator (LO_1) frequency of $2\omega_{RF}$. The magnitude of the two input signals is same with a phase difference of $\frac{\pi}{2}$.

The DC bias voltage applied between the two leads is fixed to $\frac{V_\pi}{2}$. So, V_π is the half-wave of the inner MZM-1, and it is worked in the quadrature operating point. So it is generated a SSB signal. The two leads of the lower inner-MZM-2 are biased at the minimum transmission point and it is worked by one more local oscillator (LO_2) as shown in Fig. 1. The LO2 has an angular frequency of ω_{RF}. The DC bias voltage of the inner MZM-2 is V_π.

The RF LO_1 signal is mixed with the QAM signal and can be expressed as

$$\begin{aligned} D_{RF}-QAM(t) &= V_{RF1}[I(t)\cos 2\omega_{RF}(t) - Q(t)\sin 2\omega_{RF}(t)] \\ &= \sqrt{I^2}(t)\,V_{RF1}\cos[2\omega_{RF}t+\varphi_i(t)]. \end{aligned} \tag{1}$$

Here, the amplitude of the input signal of MZM-1 is V_{RF1}. The QAM signal has two phase components as I(t) and Q(t) respectively.

As 4-QAM modulation format is used, $\sqrt{I^2(t)+Q^2}(t)=\sqrt{2}$ in Eq. (1).Where $\varphi_i(t)$ =arctan Q(t)/I(t) = $\frac{\pi}{4}$, $\frac{3\pi}{4}$, $\frac{5\pi}{4}$ and $\frac{7\pi}{4}$ for i = 1, 2, 3, and 4, respectively. The negative sidebands are suppressed due to their small amplitudes. Thus, the SSB modulated optical signal consist of two main frequencies with a spacing of $2\omega_{RF}$, a center optical frequency at ω_c and it does not carry the downlink information. The positive first-order sideband having the downlink information is at $\omega_c + 2\,\omega_{RF}$ [24]. The SSB mm-wave signal is expressed as:

$$\begin{aligned} E_{SSB}(0,t) &= \frac{\gamma_a}{2}E_c(t)\left[e^{\frac{j\pi}{V_\pi}}\sqrt{2}V_{RF1}\cos[2\omega_{RF}t+\varphi_i(t)]\right. \\ &\left. + e^{\frac{j\pi}{V_\pi}}\sqrt{2}V_{RF1}\sin[2\omega_{RF}t+\varphi_i(t)] + j\frac{\pi}{2}\right] \\ &= \frac{\sqrt{2}}{2}\gamma_a E_c e^{j\omega_c}t + m_{ha}E_c\gamma_a[(\omega_c+2\omega_{RF})t-\varphi_i(t)] \end{aligned} \tag{2}$$

Where γ_a is the insertion loss of inner-MZM-1, modulation index, $mh_a = \frac{\pi V_{RF1}}{V_\pi}$ and $J_K(.)$ is the Bessel function.

The light wave is modulated by the RF LO_2 at ω_{RF} via the inner-MZM-2. The produced carrier suppressed mm-wave signal has important first-order sidebands at $\omega_C - \omega_{RF}$ and $\omega_C + \omega_{RF}$ respectively. It is expressed as

$$\begin{aligned} E_{OCS}(t) &= \frac{\gamma_b}{2}E_c(t)\left[\left(e^{-\frac{j\pi}{V\pi}V_{RF2}}\cos(\omega_{RF}t)+j\pi\right)+e^{\frac{j\pi}{V\pi}V_{RF2}}\cos(\omega_{RF}t)\right] \\ &= \frac{\gamma_b}{2}E_{Ce^{j\omega_C}}t[\exp j(m_{hb}\cos\omega_{RF}t)\exp j(-m_{hb}\cos\omega_{RF}t)] \\ &= \gamma_b E_{C}\sum_{k=-\infty}^{\infty}[1-(-1)^k]J_k(m_{hb})e^{j(\omega_C+\omega_{RF})t+\frac{\pi}{2}} \end{aligned} \tag{3}$$

Where γ_b is the inner-MZM-2 insertion loss, and modulation index, $m_{hb} = \frac{\pi V_{RF2}}{v_\pi}$. For a value of small modulation index, $J_1^{(x)} = x$. Due to small amplitudes, the central carrier at ω_c and the higher sidebands can be neglected.

The generated Single Side Band (SSB) and carrier suppressed optical signals can be expressed as:

$$\begin{aligned} E_{D(0,t)=\gamma_{bE_Cm_{hb}}e^{j[(\omega_{C-}\omega_{RF})t}} &+ \frac{\sqrt{2\gamma_{aE_C}}}{2}e^{j\omega_C t} \\ &+\gamma_{bE_C}m_{hb}e^{j((\omega_C+\omega_{RF})t+\frac{\pi}{2})} + mh_aE_C\gamma_a e^{j(\omega_C+2\omega_{RF})t-\emptyset_i(t)} \end{aligned} \tag{4}.$$

The four optical frequencies are separated at a frequency spacing of ω_{RF}. But the frequency $\omega_c + 2\omega_{RF}$ carries the downstream data and the other frequencies are unmodulated. As the downlink data is modulated in SSB method, chromatic dispersion can be effectively reduced [23].

When the signal is transmitted through an optical fiber of attenuation coefficient, α and propagation constant, ß(ω) at an angular speed of ω. The optical signal is expressed as

$$\begin{aligned} E_D(z,t) &= \gamma_b E_C m_{hb} e^{j((\omega_c-\omega_{RF})t+\frac{\pi}{2}-\beta(\omega_c-\omega_{RF})z+\frac{\sqrt{2}}{2}\gamma_a E_C e^{j(\omega_c t} \\ &-\beta(\omega_c)z+\gamma_b E_C m_{hb}e^{j[(\omega_c+\omega_{RF})t+\frac{\pi}{2}-\beta(\omega_c+2\omega_{RF})t} \\ &-\beta(\omega_c+2\omega_{RF})z-\emptyset_1[t-[\omega_c+2\omega_{RF}]^{-1}\beta((\omega_c+2\omega_{RF})z] \end{aligned} \tag{5}$$

Figure 5 shows the BS of the multi-band access. As in Fig. 7(a)–(c), the four-band optical signal is decomposed in to three different SSB optical signals. A square law PD is generated a mm-wave signal with the principle of heterodyne beating. The RF signal

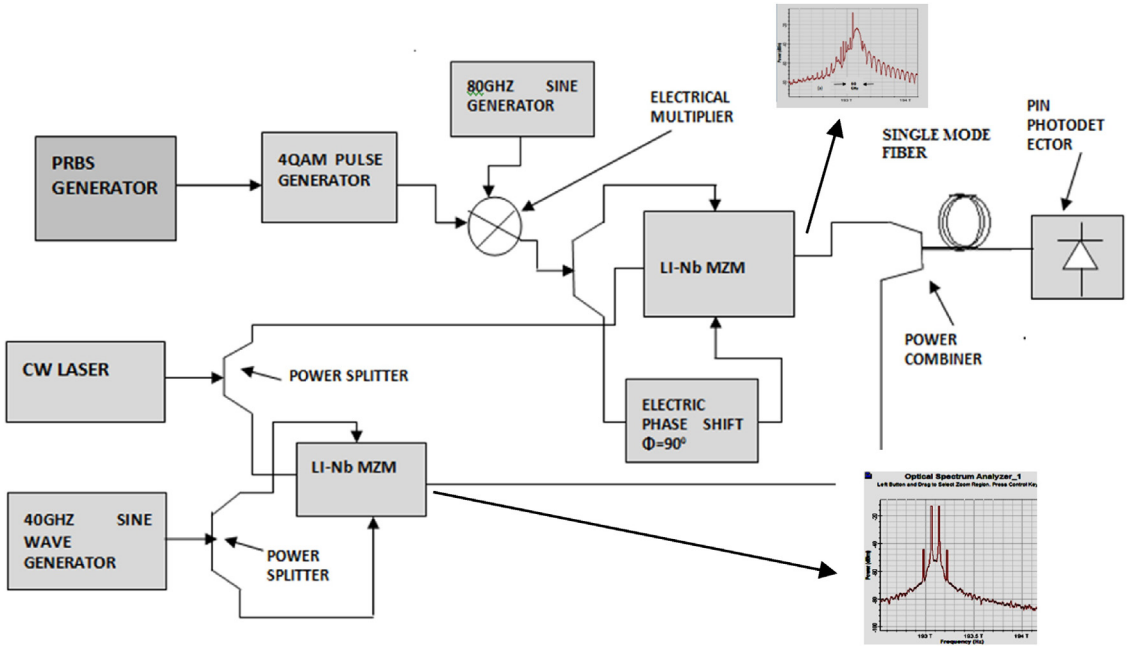

Fig. 1. Block diagram of multiband transmitter.

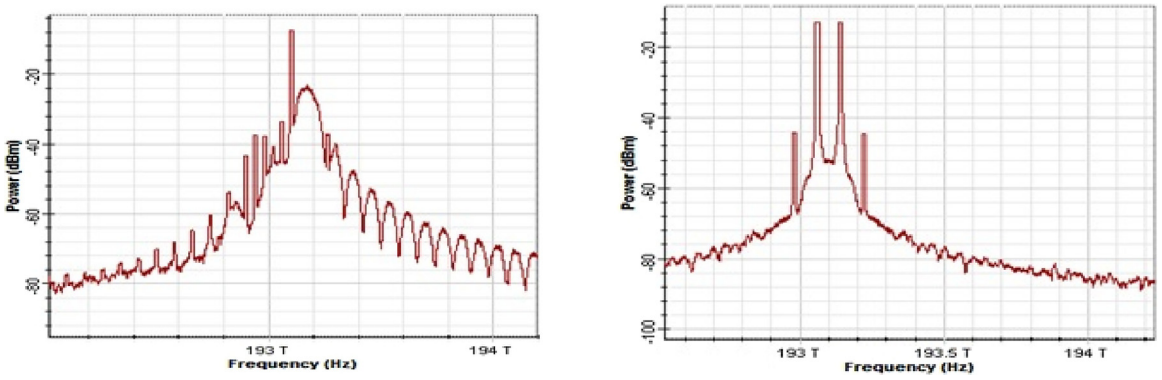

Fig. 2. (a) Optical SSB spectrum of the upper MZM. (b) RF-OCS optical spectrum of the lower MZM.

at a frequency of ω_{RF} is generated with the help of product modulator at a local oscillator frequency of ω_{RF}. The mm-wave signal at $2\omega_{RF}$ is produced by the PD and product modulator tuned with a local oscillator frequency of $2\omega_{RF}$. The mm-wave signals at $3\omega_{RF}$ is produced by tuning the local oscillator of the product modulator to $3\omega_{RF}$. The mm-wave signals are transmitted through the antenna to the user terminals for wireless transmission in the real system. The wireless signal is received by the end users and the downlink baseband data is received through coherent demodulation in the electrical domain. So, the multiband mm-wave signals are generated through our proposed method. The downlink data is modulated to a single frequency of the optical signal with SSB modulation technique. The chromatic dispersion has little effect on the generated RF signals [24].

3. Simulation Results and Discussion

Figure 1 shows the block diagram of the multiband RoF-communication system with SSB optical mm-wave signals. The optical input signal is generated from CW laser at a center frequency of 193.1 THz, a line-width of 10 MHz and an optical power of 15dBm. A power splitter is used to split this optical signal in to two beams. When these signals are applied to the inner-MZM-1 and inner-MZM-2, the SSB and carrier suppressed mm-wave signals are generated respectively. The downlink baseband 4-QAM signal is mapped by a 80 Gb/s Pseudorandom Binary Sequence (PRBS) with a word length of $2^7 - 1$. It is mixed with a 80 GHz sinusoidal wave at the upper branch of the main MZM to drive the inner-MZM-1. The inner MZM-1 has a half-wave voltage of 4 V and the DC bias voltage between the arms is 2 V. The generated SSB optical mm-wave, as in Fig. 2(a) has two optical frequencies with a resolution of 0.01 nm and a Carrier to Sideband Ratio (CSR) of 11 dB. The negative first-order sideband has a Sideband Suppression Ratio (SSR) of 8 dB and due to small amplitudes, higher sidebands can be avoided. The carrier suppressed output at the lower MZM-2 is shown in Fig. 2(b).

As in Fig. 2(a), unmodulated optical frequency is at central carrier of 193.1 THz and the positive first-order sideband frequency is at 193.18 THz. The sidebands have a frequency spacing of 80 GHz. The second arm of the central MZM is modulated by a 40 GHz RF frequency and a driving voltage of 1 V through the inner-MZM-2. It is biased at the minimum transmission operating point with a half-wave voltage of 4 V and the DC bias voltage of 4 V. As in Fig. 2(b), the even order sidebands and the optical carrier can be suppressed completely. The remaining high-order sidebands have amplitudes 32 dB lower than the first order sidebands as in the optical spectrum. From Fig. 2(b), the two sidebands at 193.06 THz

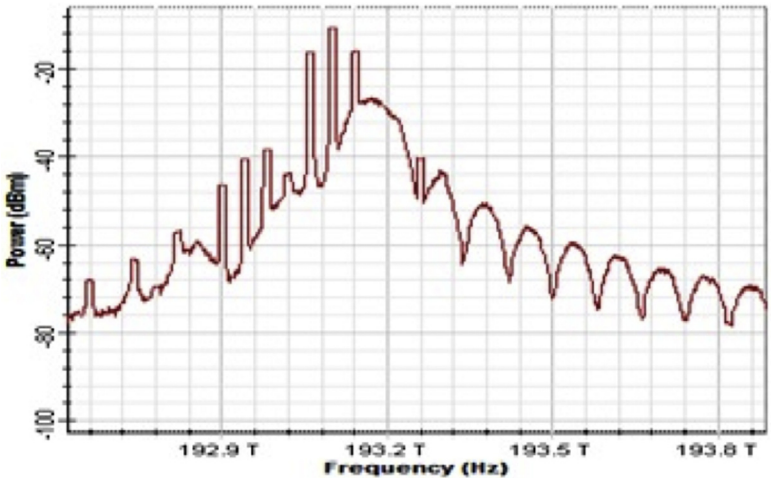

Fig. 3. Generated optical spectrum of the main MZM.

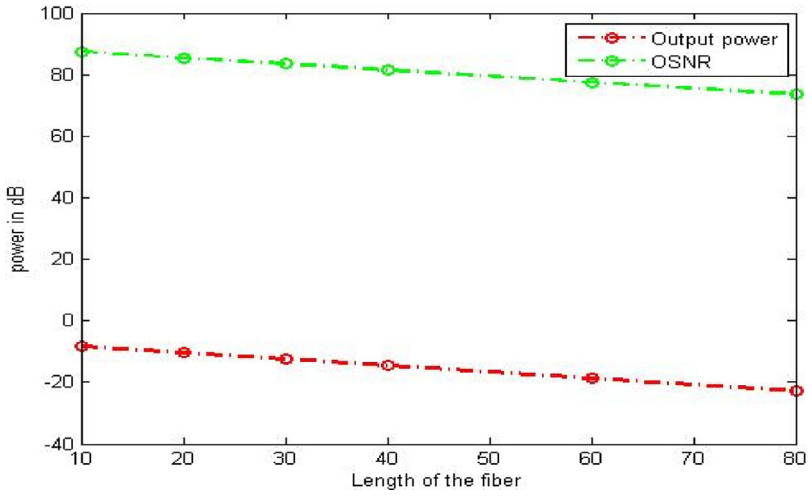

Fig. 4. Output optical power and OSNR of the generated optical millimeter wave for different length of fiber (Km).

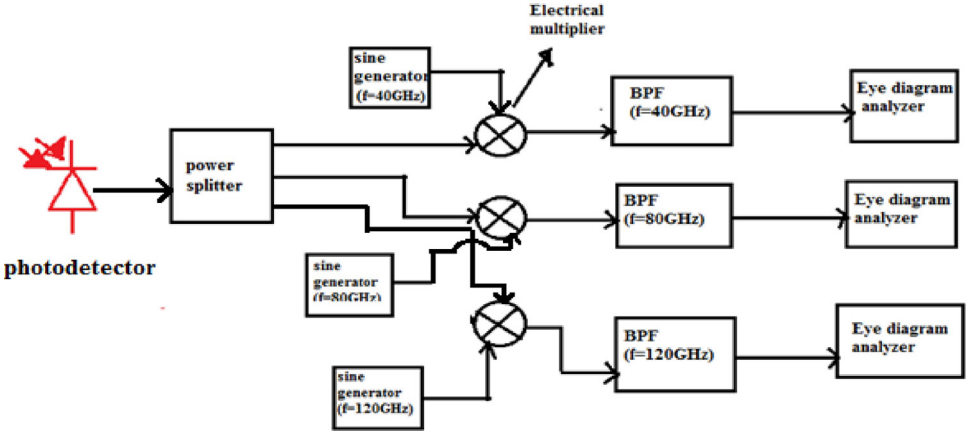

Fig. 5. Block diagram of multiband base station.

and 193.14 THz have a frequency spacing of 80 GHz. The optical signal consists of a SSB modulated signal from the upper branch and a carrier suppressed optical signal from the lower branch. An optical bandpass filter (OBPF) at a central frequency of 193.1 THz and bandwidth of 100 GHz is used to remove the smaller sidebands and noises. Figure 3 mainly contains a spectrum of four tones in which the frequency of 193.18 THz carries the downlink data and the other tones are unmodulated frequencies. The generated multiband is transmitted to the BS through a Single Mode Fiber (SMF). It has a chromatic dispersion of 16.75 ps/nm/Km, a power attenuation of 0.2 dB/Km and a dispersion slope of 0.075 ps/nm ^{2}/km. Figure 4 shows the OSNR and output optical power of the mm-wave trans-

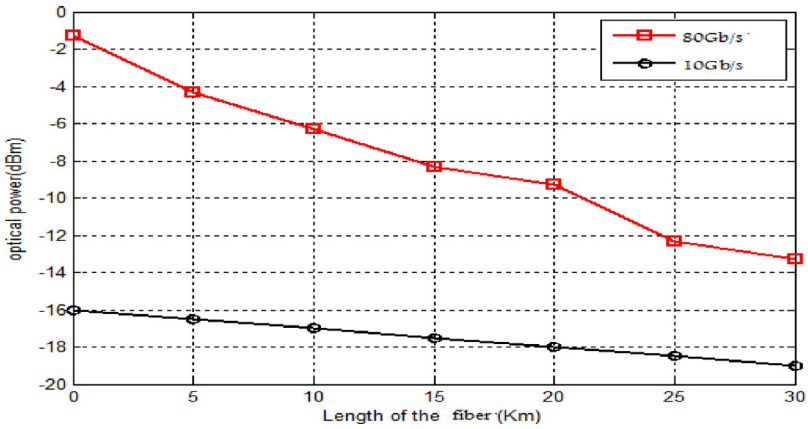

Fig. 6. Output optical signal power of millimeter wave at data rates of 80 Gb/s and 10 Gb/s respectively.

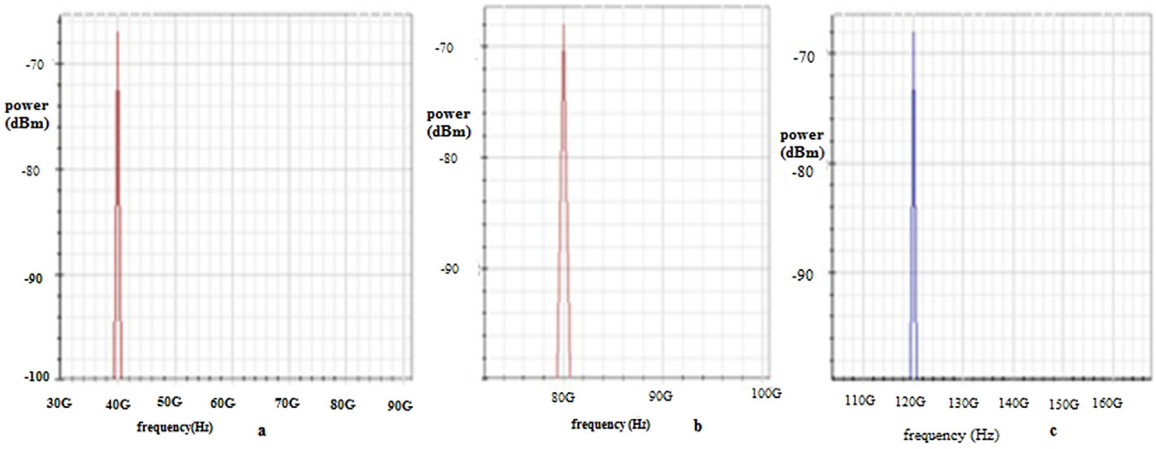

Fig. 7. Received electrical spectra of millimeter waves at (a) 40 GHz (b) 80 GHz (c) 120 GHz.

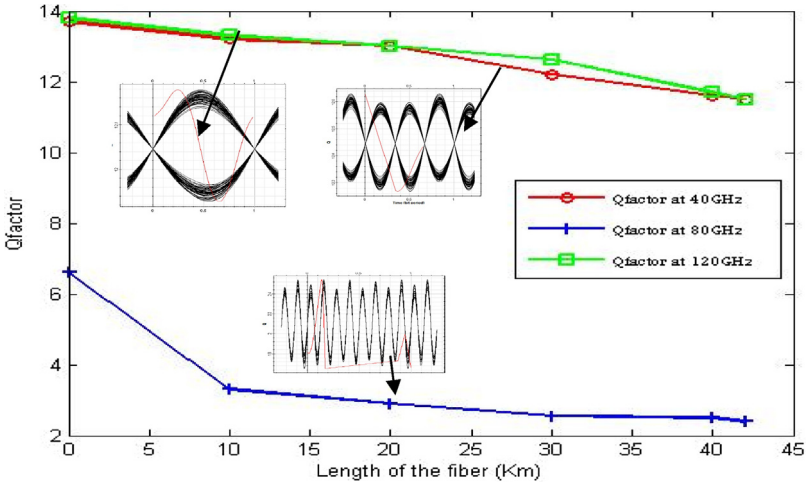

Fig. 8. Q-factor and eye diagram performance of the received mm waves for frequencies 40 GHz, 80 GHz and 120 GHz.

mission. Figure 5 shows the block diagram of the multiband base station.

At the BS, the optical signal is directly injected into a PD with a responsivity of 1 mA/mW, dark current and thermal noise of the PD are 10 nA and $1e^{-22}$ W/Hz, respectively. The electrical signal is applied to a product modulator. For the 80 GHz mm-wave generation, the local oscillator is adjusted to 80 GHz and the unwanted sidebands are avoided with an electrical band-pass RC filter at a cutoff frequency of 80 GHz. The 40 GHz signal can be generated by a local oscillator with a cut-off frequency of 40 GHz. The 120 GHz signal is generated by a local oscillator frequency of 120 GHz. The unwanted sidebands are reduced by using a band pass RC filter with a cut-off frequency of 120 GHz. Figure 6 shows the difference of optical received signal power of RF waves for 80 Gb/s (proposed method) and 10 Gb/s(existing method). For both methods, the signal power decreases with increasing transmission distances.

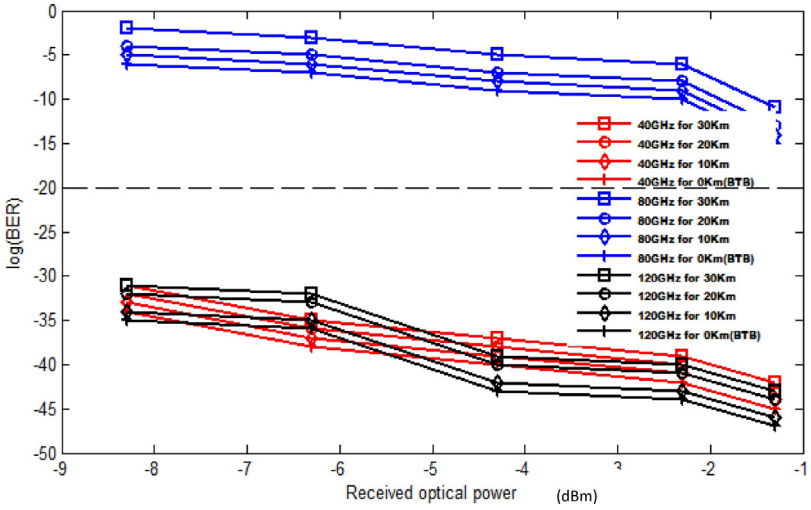

Fig. 9. BER performances of 40 GHz, 80 GHz and 120 GHz millimeter wave signals at B-T-B, 10 Km, 20 Km and 30 Km of fiber length.

The signal power has a maximum shift of 15 dB from the existing method. The output signal spectrums of three frequency bands are shown as in Fig. 7(a)–(c) respectively. Figure 8 shows the Q-factor and eye diagrams of 40 GHz, 80 GHz and 120 GHz millimeter waves. For 40 GHz and 120 GHz, the eyes are more closed with minimum noises and high Q factors. But for 80 GHz, the eye diagram is not closed, and Q Factor is below 6 dB except BTB transmission. So the performance of 80 GHz is worse than other two bands.

Figure 9 shows the graph between the measured BER and received optical power of the 80 Gb/s 4QAM signal for the mm-wave signals of 40 GHz, 80 GHz and 120 GHz respectively. Their performances are analyzed for the transmission distance of 0 Km (B-T-B), 10 Km, 20 Km and 30 Km, respectively. Graphs show that the BER is gradually decreased with increase in optical powers. Results show that 80 GHz mm-wave shows worse performance in compared to others. The 120 GHz band shows best performance and performance of the 80 GHz band is in between 40 GHz and 80 GHz. The 80 GHz band shows worst performance due to low Q factor as in Fig. 8. As the chromatic dispersion is low, B-T-B transmission shows best performance in three-millimeter bands.

The proposed method shows a novel technique of a higher multiband mm-wave transmission for a higher data rate of 80 Gb/s. The signal decomposition technique at the BS can reduce the nonlinearities due to FBGs. Besides, the received optical power is greater than −4 dBm with a lower BER about 10^{-20} even for a fiber length of 30 Km.

4. Conclusions

We have presented a novel low-cost RoF communication system with SSB modulated mm-wave signal to carry the 40 GHz, 80 GHz and 120 GHz multiband mm-wave wireless communication. This proposed method uses a simple signal decomposition technique instead of using FBGs and optical filters in the existing method. So the proposed low-cost method is reduced the nonlinearities in the FBGs. The simulation results reveal that our proposed method is performed a multiband mm-wave transmission at a data rate of 80 Gbps with higher transmission performances in terms of low BER, higher Q factor and higher received optical power. Results show that BER is around 10^{-20} with a large output optical power of −4 dBm even at a SMF length 30 Km. The results indicate that the proposed method can provide better performance in multiband RoF communication.

References

[1] R.C. Daniels, R.W. Heath, 60 GHz wireless communications: emerging requirements and design recommendations, IEEE Veh Technol. Mag. 2 (September (3)) (2007) 41–50.
[2] A.M.J. Koonen, L.M. Garcia, Radio-over-MMF techniques-part II: microwave to millimeter-wave systems, J. Lightw. Technol. 26 (August (15)) (2008) 2396–2408.
[3] J.J. Vegas Olmos, T. Kuri, K. Kitayama, Dynamic reconfigurable WDM 60-GHz millimeter-waveband radio-over-fiber access network: architectural considerations and experiment, J. Lightw. Technol. 25 (November (11)) (2007) 3374–3380.
[4] S.-H. Lee, H.-J. Kim, J.-I. Song, Broadband photonic single sideband frequency up-converter based on the cross polarization modulation effect in a semiconductor optical amplifier for radio-over-fiber systems, Opt. Express 22 (January (1)) (2014) 183–192.
[5] Ch.-H. Ho, Ch.-T. Lin, Y.-H. Cheng, H.-T. Huang, C.-C. Wei, S. Chi, High spectral efficient W-band optical/wireless system employing single-sideband single-carrier modulation, Opt. Express 22 (February (4)) (2014) 3911–3917.
[6] K. Ikeda, T. Kuri, K. Kitayama, Simultaneous three-band modulation and fiber-optic transmission of 2.5-Gb/s baseband, microwave-and 60-GHz-band signals on a single wavelength, J. Lightw. Technol. 21 (December (12)) (2003) 3194–3202.
[7] C. Qingjiang, F. Hongyan, S. Yikai, Simultaneous generation and transmission of downstream multiband signals and upstream data in a bidirectional radio-over-fiber system, IEEE Photon. Technol. Lett. 20 (February (3)) (2008) 181–183.
[8] S. Mikroulis, O. Omomukuyo, M.P. Thakur, J.E. Motchell, Investigation of an SMF-MMF link for a remote heterodyne 60 GHz OFDM RoF-based gigabit wireless access topology, IEEE J. Lightw. Technol. 32 (May) (2014) 3645–3653.
[9] T. Kamisaka, T. Kuri, T. kitayama, Simultaneous modulation and fiber optic transmission of 10 Gbps baseband and 60 GHz band radio signals on a single wavelength, IEEE Trans. Microw. Technol. 49 (October (10)) (2001) 2013–2017.
[10] K. Ikeda, T. Kuri, K. Kitayama, Simultaneous three-band modulation and fiber-optic transmission of 2.5-Gb/s baseband, microwave-, and 60-GHz-band signals on a single wavelength, J. Lightw. Technol. 21 (December (12)) (2003) 3194–3202.
[11] J.J. Vegas Olmos, T. Kuri, K. Kitayama, Reconfigurable radio-over-fiber networks: multiple-access functionality directly over the optical layer, IEEE Trans. Microw. 11 (October (11)) (2010) 3001–3010.
[12] L. Zhang, X.-F. Hu, P. Cao, Q. Chang, Y. Su, Simultaneous generation of independent wired and 60-GHz wireless signals in an integrated WDM-PON-RoF system based on frequency-sextupling and OCS-DPSK modulation, Opt. Express 20 (13) (2012) 14648–14655.
[13] I. Aldaya, G. Campuzano, C. G, G. Castanon, Simultaneous generation of wavelength division multiplexing PON and RoF signals using a hybrid mode-locked laser, Opt. Fiber Technol. 23 (June) (2015) 53–60.
[14] M. Bakaul, A. Nirmalathas, C. Lim, D. Novak, Hybrid multiplexing of multiband optical access technologies towards an integrated DWDM network, IEEE Photon. Technol. Lett. 18 (November (21)) (2006) 2311–2313.
[15] Q. Chang, H. Fu, Y. Su, Simultaneous generation and transmission of downstream multiband signals and upstream data in a bidirectional radio-over-fiber system, IEEE Photon. Technol. Lett. 18 (21) (2008) 181–183.
[16] Q. Chang, H. Fu, Y. Su, Simultaneous generation and transmission of downstream multiband signals and upstream data in a bidirectional radio-over-fiber system, IEEE Photon. Technol. Lett. 20 (February (3)) (2008) 181–183.

[17] Z. Jia, J. Yu, Y.-T. Hsueh, A. Chowdhury, Multiband signal generation and dispersion-tolerant transmission based on photonic frequency tripling technology for 60-GHz radio-over-fiber systems, IEEE Photon. Technol. Lett. 20 (September (17)) (2008) 1470–1472.
[18] Y.-T. Hsueh, Z. Jia, H.-Ch. Chien, A. Chowdhury, Multiband 60-GHz wireless over fiber access system with high dispersion tolerance using frequency tripling technique, EEE J. Lightw. Technol. 29 (April (8)) (2011) 1105–1111.
[19] Y.-T. Hsueh, Z. Jia, H.-C. Chien, J. Yu, G.-K. Chang, A novel bidirectional 60-GHz radio-over-fiber scheme with multiband signal generation using a single intensity modulator, IEEE Photon. Technol. Lett. 21 (September (18)) (2009) 1338–1340.
[20] Ch.-Y. Li, H. Su, Ch.-H. Chang, H.-H. Lu, Generation and transmission of BB/MW/MMW signals by cascading PM and MZM, J. Lightw. Technol. 30 (February (3)) (2012) 298–303.
[21] H. Kumazaki, Y. Yamada, H. Nakamura, S. Inaba, Tunable wavelength filter using a Bragg grating fiber thinned by plasma etching, IEEE Photon. Technol. Lett. 13 (November (11)) (2001) 1206–1208.
[22] Z. Li, V.K.S. Hsiao, Z. Chen, J.Y. Tang, Optically tunable fiber Bragg grating, IEEE Photon. Technol. Lett. 22 (May (15)) (2010) 1123–1125.
[23] S. Choi, T. Eom, Y. Jung, B. Lee, Broad-band tunable all-fiber bandpass filter based on hollow optical fiber and long-period grating pair, IEEE Photon. Technol. Lett. 17 (January (1)) (2005) 115–117.
[24] R. Zhang, J. Ma, W. Liu, W. Zhou, Y. Yang, A multi-band access radio-over-fiber link with SSB optical millimeter-wave signals based on optical carrier suppression modulation, Opt. Switch. Netw. 18 (September) (2015) 235–241.